

# Effect of Carbon preform architecture on the Mechanical and Thermal Properties of 4D Carbon/Carbon Composites

H. J. Joo, Z. B. Kim, and K. W. Lee, Chungnam National University, Daejeon 305-764, Korea

## Abstract

The mechanical and thermal properties of 4D carbon/carbon composites have been studied with four kinds of carbon preform. In this study, the fabricated preforms that were prepared four different bundle spacing were used. The preforms were densified using the molten pitch impregnation and carbonization process and the densified block was graphitized. A three-point bending test was used to investigate the influence of bundle spacing of the preform on the flexural properties and microstructure of the composites. And coefficient of thermal expansion and thermal conductivity with direction of reinforced fiber were investigated.

## Introduction

Carbon fiber reinforced carbon (C/C) composites are regarded as one the best thermal structural materials owing to their light weight, high strength and modulus even at high temperature, excellent thermal shock resistance. These advantages of the composites in comparison with ceramics and metals have let the composites in the field of aerospace applications. The composites with uni-directional (UD) and two-directional (2D) fabric perform have been extensively investigated. They exhibit strong anisotropy since the arrangement of fibers in the perform is anisotropic. To improve on the extreme anisotropy of C/C composite, multidirectional (nD) perform was devised in the space flight fields. The properties of the finished nD composite in terms of density, mechanical or thermal characteristics will depend on a number of factors such as; the type of carbon fiber used, the size of the fiber bundle, the spacing of the tows and the angles of the tows relative to the axes of the perform.

In this paper, four kinds of 4D reinforced preforms with different spacing of the tows were prepared, and 4D C/C composites were fabricated using the molten pitch impregnation/carbonization and the densified blocks were graphitized. Then the influence of bundle spacing in the perform on the mechanical and thermal properties are discussed.

## Experimental

### Composite preparation

The perform used to fabricate C/C composites was prepared by weaving method. It was hexagonal shape with four directional axis; W, X and Y plane layer were stacked to be cross over at 120°, and Z axes was perpendicular to W, X and Y plane (as depicted in Figure 1). A diameter of the hole in weaving tool was controlled to be 1.7 to 4.0 mm and distance between the holes to be 1.2 to 2.0 mm. The carbon fiber was used PAN based TZ-307 from Taekwang Co. (Korea) and coal tar pitch was used as matrix-precursor.

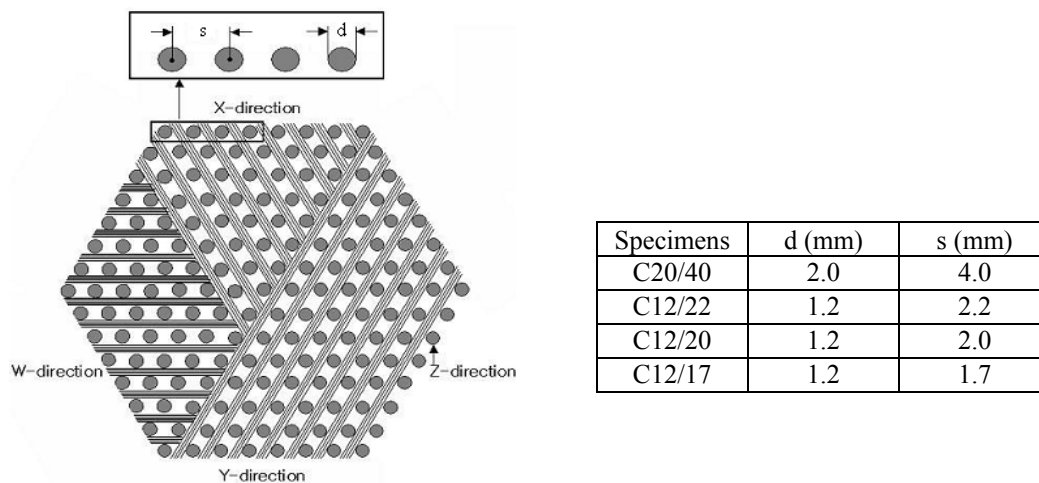


Figure 1. Schematic diagram of cross-section of Z-axis direction of 4D carbon preform.

Preparation of C/C composites requires many repeated densification cycles. This includes pressure impregnation and carbonization (PIC) and graphitization to achieve the desired density. The PIC process was performed as follows; high pressure impregnation with coal tar pitch at 60 MPa and 300 °C, after that heat treatment up to 650 °C under 60 MPa. Finally, the carbon billets were graphitized at 2300 °C.

### Thermal test

The laser flash method was used to measure the thermal diffusivity of the C/C composites. The measurements were carried out from 25 °C to 900 °C in argon on disk shaped specimens with a diameter of 12.5 mm and thickness of 2.5 mm. Specimens were tested both X axes and Z axes direction to the fibre array. The thermal conductivity of the specimens was calculated by the following formula;

$$\alpha = c \cdot \lambda \cdot \rho$$

where,  $c$  and  $\lambda$  is specific heat and thermal diffusivity, and  $\rho$  is density (at 25 °C) of the specimens. To measure coefficient of thermal expansion a dilatometer equipped with silica tube and push rods was used. The dimensions of specimens were rod shaped with a diameter of 5 mm and a length of 25 mm. The tests were performed in nitrogen atmosphere at heating rate of 10 °C/min from 25 °C to 1000 °C.

### Three-point bending test

The specimens were prepared to be dimension of  $90 \times 8 \times 6 \text{ mm}^3$ . The distance of support span was 80 mm and cross-head speed was 1.0 mm/min. Flexural strength (S) and modulus (E) were calculated by the following equations;

$$S = \frac{3PL}{2bd^2} \quad E = \frac{0.25L^3m}{bd^3}$$

Where, L is the distance of span, d is the thickness of specimen, b is the width and m is the slope of the straight of the load/displacement curve.

## Results and discussion

Carbon matrix tend to be closely formed inside of fiber bundles which are densely composed with fibres, on the other hand, there are a lot pores and cracks in matrix pockets which means space where fiber bundles cross over. Moreover, serious cracks are observed at interface of each bundle as well as where bundles and matrix pockets meet. These cracks are occurred during densification process and pores may come from decomposition gas or volatilization caused by carbonization of pitch. Both of them appear less when unit cells of perform are smaller.

**Table 1.** Specifications of carbon/carbon composites.

| Number of specimens | Fiber volume fraction (%) |        | Distance between X and Y (or W) direction layer (mm) | Preform density (g/cm <sup>3</sup> ) | Size of bundle (K) |       | Bulk density of C/C (g/cm <sup>3</sup> ) |
|---------------------|---------------------------|--------|--|--------------------------------------|--------------------|-------|--|
|                     | Total                     | X<br>Z |  |                                      | X<br>Z             |       |  |
| C20/40 (1)          | 41.2                      | 8.55   | 3.4  | 0.738                                | 24                 | 1.861 |  |
|                     |                           | 15.56  |  |                                      | 48                 |       |  |
| C20/40 (2)          | 47.8                      | 10.76  | 5.7  | 0.855                                | 48                 | 1.837 |  |
|                     |                           | 15.48  |  |                                      | 48                 |       |  |
| C12/22 (1)          | 38.8                      | 9.36   | 2.8  | 0.644                                | 12                 | 1.817 |  |
|                     |                           | 10.69  |  |                                      | 12                 |       |  |
| C12/22 (2)          | 50.5                      | 8.90   | 3.0  | 0.905                                | 12                 | 1.876 |  |
|                     |                           | 23.84  |  |                                      | 24                 |       |  |
| C12/20 (1)          | 35.8                      | 7.29   | 3.8  | 0.627                                | 12                 | 1.875 |  |
|                     |                           | 13.90  |  |                                      | 12                 |       |  |
| C12/20 (2)          | 50.3                      | 7.82   | 3.6  | 0.900                                | 12                 | 1.854 |  |
|                     |                           | 26.82  |  |                                      | 24                 |       |  |
| C12/17              | 53.2                      | 4.85   | 3.6  | 0.952                                | 12                 | 1.817 |  |
|                     |                           | 38.64  |  |                                      | 24                 |       |  |

From the stress-displacement curves in Figure 6, it was observed that the fracture behavior of the composites were exhibited an obvious pseudo-plastic fracture. In especially, X direction of the composites were showed excellent toughness even though it had been included low fibre volume fraction. The most curves could be divided into three regions; the first applied stress increases linearly with an increment of displacement, second when the stress arrives at a certain value, the specimens start the pseudo-plastic deformation until stress get the maximum point, then stepwise failure occurs.

Flexural strength and modulus of Z direction of the composites were increased with an increment of the reinforced fiber volume fraction. But those of X direction weren't depended on the fiber volume fraction. By comparing flexural properties of all specimens in Figure 3, specimen C12/17 is possessed the highest flexural strength and modulus though it was included the lowest reinforced fiber volume fraction.

As showing the microstructure of the composites in Figure 2, specimen C12/17 was consisted of the smallest unit cell. Consequently, it has smallest matrix pocket including smaller pores and apertures. In order words, specimen C12/17 is compact and homogeneous in texture compare with the others, and exhibits superior flexural strength and modulus.

The thermal conductivity of the composites, in both direction of X and Z axis bundles, is indicated in Figure 7. Their thermal conductivity was increased with reinforced fiber volume fraction and rising temperature. That of specimen C12/17 in X direction is the second highest though it was reinforced with the lowest fiber volume fraction. In Z direction, it is outstandingly high thermal conductivity compare with the others. These results is caused by homogeneous texture in the composites.

The effect of the preform architectures on the coefficient of thermal expansion for the composites is shown in Figure 8. The thermal expansion responses of X and Z direction were exhibited a negative value up to around 400 °C, and positive response at higher temperature. When the unit cell of the composite is smaller, the range of negative thermal expansion is more extended, and lower coefficient of thermal expansion is exhibited.

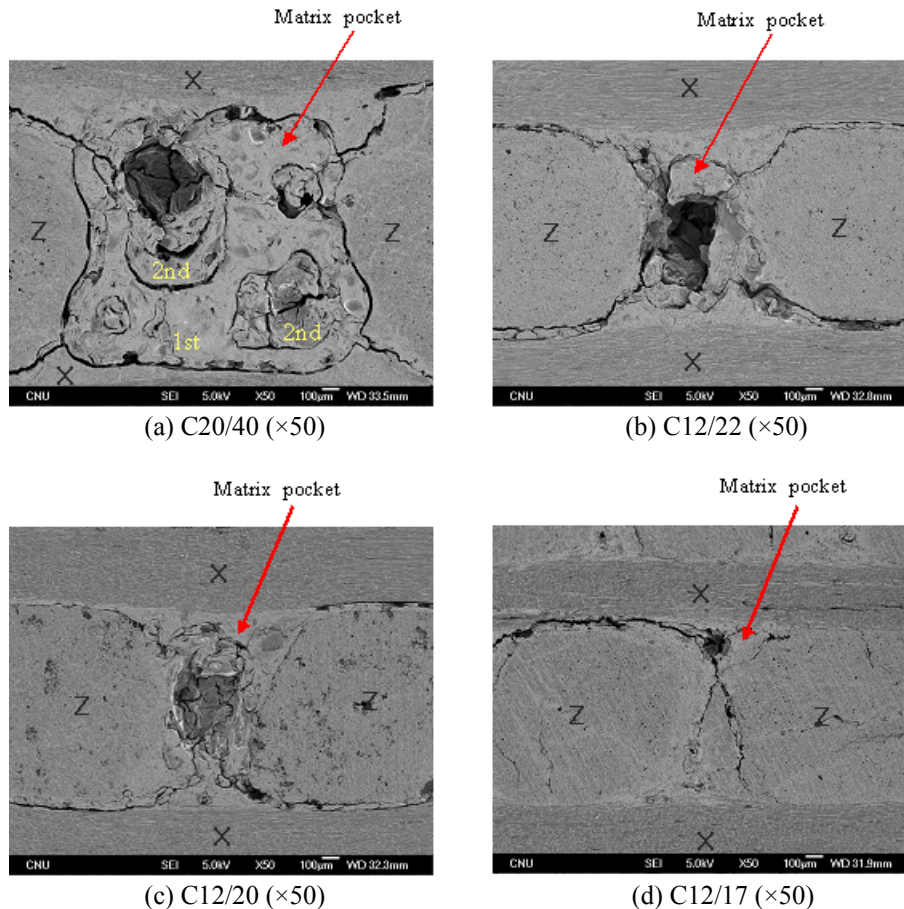


**Figure 2.** SEM photographs of matrix-pocket between fiber bundles in 4D C/C composites.

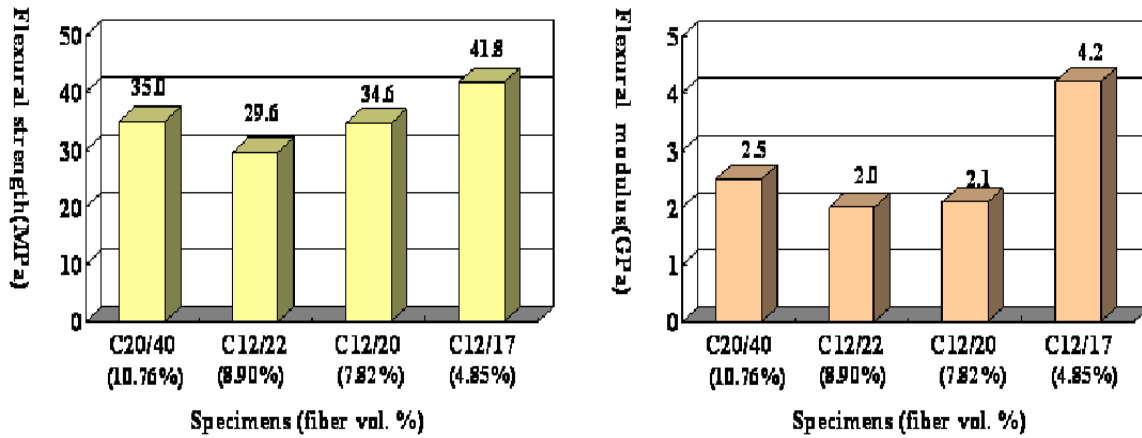


Figure 3. Flexural strength and modulus of X-direction of 4D C/C composites.

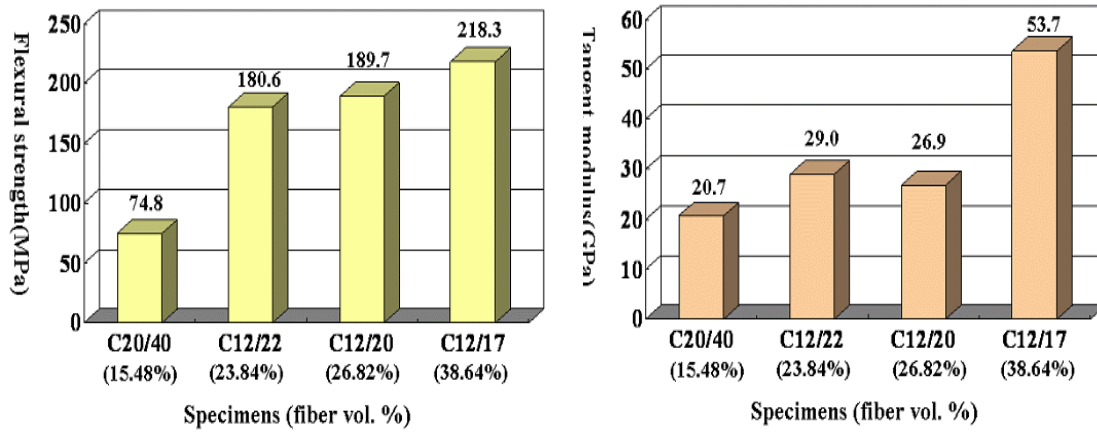


Figure 4. Flexural strength and modulus of Z-direction of 4D C/C composites.

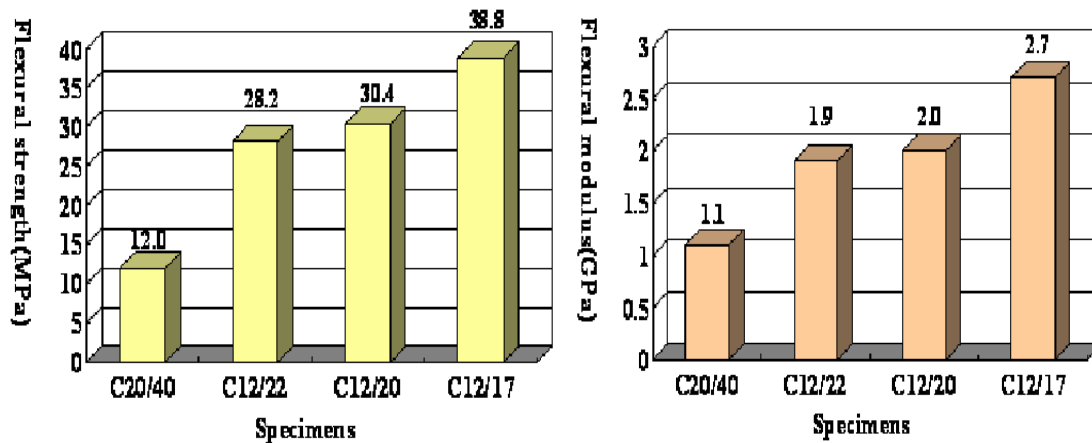
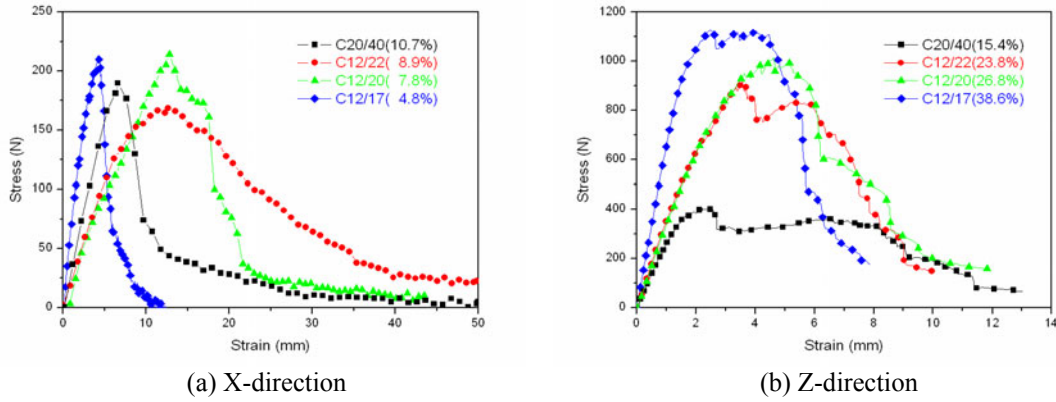
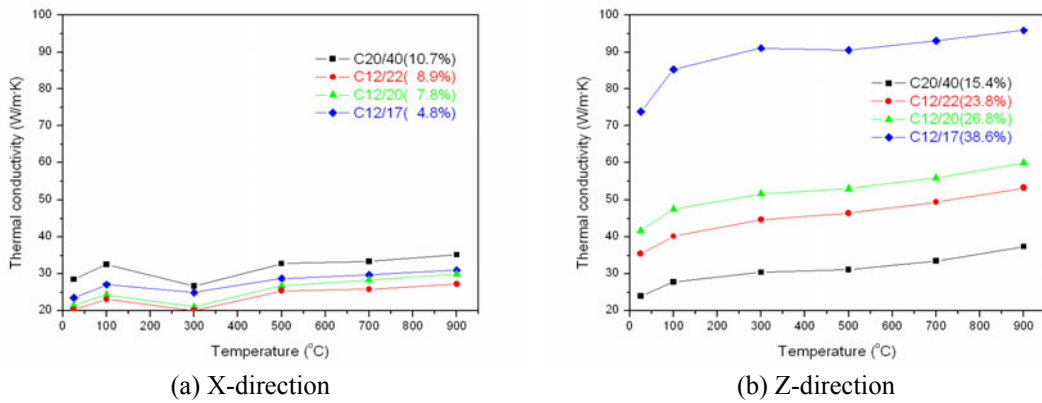


Figure 5. Flexural strength and modulus of perpendicular direction to X axis in 4D C/C composites.



**Figure 6.** Stress-strain curves of C/C composites under flexural loading.



**Figure 7.** The temperature dependence of thermal conductivity of 4D carbon/carbon composites.

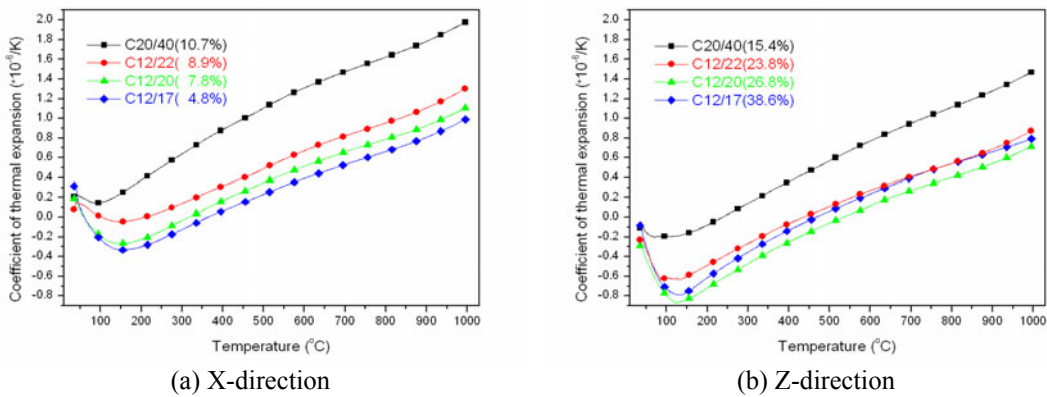


**Figure 8.** The temperature dependence of thermal expansion coefficient of 4D carbon/carbon composites.

### Conclusions

The size of unit cell of the preforms has considerably affected on the mechanical and thermal properties as well as microstructure of the 4D carbon/carbon composites. While the carbonization and graphitization process, contraction were happened more equally when unit cell are smaller and it trigger superior mechanical properties as the reinforced fibres get less damage. Even though carbon matrix start graphitized, their thermal conductivity still could be depended on fiber volume fraction. In addition, dispersion of reinforced fibre are more uniform (unit cell of preform is smaller), it appears that thermal

conductivity was increased and coefficient of thermal expansion was decreased. One particular thing has to be pointed out is that their fractural behaviors seem to be quite tough motion compare with typical carbon/carbon composites. It is assumed that this phenomenon is occurred by that preform are woven and the straightness of fibre bundles become less intense.

### *References*

- Fitzer, E., Hüttinger, W., and Manocha, L.M. 1980. Influence of process parameters on the mechanical properties of carbon/carbon-composites with pitch as matrix precursor. *Carbon* 18:291-295.
- Buckley, J.D. 1988. Carbon-Carbon: an overview. *American Ceramic Society Bulletin* 67:364-368.
- Fitzer, E., Gkogkidis, A., and Heine, M. 1984. Carbon fibres and their composites. *High Temperatures and High Pressures* 16:363-392.
- Luo, R.Y. 2002. Friction performance of C/C composites prepared using rapid directional diffused CVI processes. *Carbon* 40:1279-1285.
- Siron, O., Chollon, G., Tsuda, H., Yamauchi, H., Maeda, K., and Kosaka, K. 2000. Microstructural and mechanical properties of filler-added coal-tar pitch-based C/C composites: the damage and friction process in correction with AE wave form parameters. *Carbon* 38:1369-1389.
- Fitzer, E. 1987. The future of carbon-carbon composites. *Carbon* 25:163-190.
- Siron, O. and Lamon, J. 1998. Damage and failure mechanisms of a 3-D Carbon/Carbon composites under uniaxial tensile and shear loads. *Acta Materialia* 46:6631-6643.
- Fei, Y.Q., McEnaney, B., Derbyshire, F.J., and Burchell, T.D. 1993. Microstructural characterization of 3D Carbon-Carbon composites, 1. A systematic Observation of structure by SEM. Pages 64-65, *21<sup>st</sup> Biennial Conference on Carbon*. State University of New York, Buffalo, USA.